JOURNAL OF MATERIALS SCIENCE: MATERIALS IN MEDICINE 15 (2004) 803–808

Bioactive evaluation of 45S5 bioactive glass fibres and preliminary study of human osteoblast attachment

DANIEL C. CLUPPER, JULIE E. GOUGH*, PAPY M. EMBANGA, IOAN NOTINGHER, LARRY L. HENCH
Department of Materials, Imperial College London, South Kensington Campus, London, SW7 2BP, UK
E-mail: j.gough@umist.ac.uk

MATTHEW M. HALL
Department of Ceramic Engineering and Materials Science, Alfred University, Alfred, New York, 14802, USA

Bioactive glass fibres can be used as tissue engineering scaffolds. In this investigation, the bioactive response of 45S5 glass fibres was assessed in simulated body fluid (SBF). Preliminary attachment of osteoblasts to the fibre surface was assessed, as were the fibre tensile strength and fracture toughness. Fourier transform infrared spectroscopy (FTIR) analysis revealed that hydroxyapatite (HA) was formed on the fibres' surface after 2–4 days in SBF. Raman micro-spectroscopic analysis was used to monitor development of the HA layer during immersion. A correlation was found between increase in intensity of the PO_4^{3-} peak near 964 cm^{-1} and appearance of crystalline HA (P–O bending peaks) using FTIR. Such results are encouraging for *in situ* bioactivity monitoring, as Raman spectra are insensitive to the presence of water, unlike FTIR. Average tensile strength of 45S5 fibres (79 μm diameter) was 340 $\pm$ 140 MPa. Fracture toughness, determined using fracture surface analysis, was 0.7 $\pm$ 0.1 MPa $m^{1/2}$. Confocal microscopy revealed osteoblasts attached and spread along the fibres after 15–90 min culture. Scanning electron microscopy analysis showed that cells with filopodia and dorsal ruffles remained attached after 14 days in culture. These results are encouraging, as cell adhesion is an important first step prior to proliferation and differentiation.

1. Introduction

Bioactive glass 45S5 is well suited for repairing bone defects in low-load bearing areas *in vivo* [1–5]. The hydroxyapatite (HA) surface layer that forms in aqueous solution plays a significant role in forming a strong bond with bone [6–8]. *In vitro* work has shown that bioactive glass 45S5 stimulates osteoblasts to proliferate, differentiate, and to lay down an extracellular matrix at the bioactive glass surface [9–12]. Furthermore, the ionic dissolution products of 45S5 glass alone stimulate osteoblast proliferation *in vitro* [13] by causing up-regulation of genes related to growth and cell cycle regulation [14].

There is much interest in bioactive fibres for tissue engineering scaffolds [15–19]. However, crystallisation of fibres can have deleterious effects on fibre production and the mechanical properties. Furthermore, crystallisation can also slightly decrease the bioactivity. Glasses such as 45S5, with high Ca and Na oxide contents have traditionally been difficult to produce in fibrous form due to ease of crystallisation. Therefore, attempts have been made to avoid crystallisation either by alternative processing methods (such as sol–gel) or by altering the melt composition (e.g. by taking advantage of the mixed alkali effect).

A variety of cells (bone, lung, etc.) can be cultured onto fibres or a fibrous meshwork for in-depth study of cellular reaction to these bioactive scaffolds. An open mesh structure facilitates tissue ingrowth and diffusion of nutrients and waste products. In addition, degradable bioactive glass fibres are used as reinforcement for resorbable composites [20, 21] and have been proposed for use in biosensor applications [22].

Although several forms of bioactive glass 45S5 have been studied, such as monoliths, particulates, and porous materials, published data on the mechanical properties, bioactivity, and *in vitro* osteoblast response to 45S5 glass fibres is sparse [23]. This investigation reports on the

*Author to whom all correspondence should be addressed: Manchester Materials Science Centre, UMIST and the University of Manchester, Grosvenor Street, Manchester M1 7HS, UK.

bioactivity, strength and toughness, and preliminary attachment of osteoblasts to fibrous bioactive glass 45S5.

2. Methods and materials

2.1. Fibres and bioactivity testing

Bioactive 45S5 glass fibres with nominal composition 46.1% (mol) SiO_2, 26.9 CaO, 24.4 Na_2O, and 2.5 P_2O_5 were obtained commercially (MO-SCI Corporation, Rolla, MO, USA) in 20 and 40 μm diameters. In addition, larger (150–300 μm) 45S5 fibres were also hand-drawn from the melt by the authors.

Bioactivity testing was carried out by immersing 20 and 40 μm diameter fibres in simulated body fluid (SBF) (142.0 mM Na^+, 5.0 K^+, 1.5 Mg^{2+}, 2.5 Ca^{2+}, 148.8 Cl^-, 4.2 HCO_3^-, 1.0 HPO_4^{2-} at pH 7.25 [24]) at 37 °C for time periods ranging from 30 min to 20 days. Approximately 0.0532 g of 40 μm fibres or 0.0266 g of 20 μm fibres were immersed in 20 ml SBF and shaken at 175 rpm. Each of these reactivity experiments corresponded to a fibre surface area to solution volume ratio of approximately 1.0 cm^2/ml (2 cm fibre lengths). Following immersion, fibres were rinsed with acetone and dried at 60 °C.

Fourier transform infrared spectroscopy (FTIR) was performed using a Spectronic Unicam Genesis II after mixing fibre samples with KBr (1 : 100 by wt). Analysis was performed in reflectance mode between 1400 and 400 cm^{-1} in order to characterise the formation of a HA surface layer.

Raman spectra were recorded using a Renishaw 2000 micro-spectrometer equipped with a 100 mW power (at sample) 830 nm diode laser. The laser beam was focused using a Leica 50 × /0.75 objective, the same objective being used also for the collection of Raman signal. The spectra were recorded for 10 s and 10 spectra were averaged.

2.2. Strength and toughness assessment

Hand-drawn bioactive 45S5 fibres ($n = 44$) were mounted using a 20 mm gauge length on heavy grade paper (230 gsm, Ryman Ltd., UK) using an epoxy resin (Araldite®, Bostik Ltd., UK). Prior to testing, the resin mounting of the fibres was cured for three days at 60 °C. The crosshead displacement rate during testing was 0.5 mm/min.

Scanning electron microscopy (SEM) (JEOL T-220A) was used in the examination of the fibre fracture surfaces. The fracture toughness (K_{IC}) was calculated using

$$K_{IC} = 1.24\sigma\sqrt{c} \quad (1)$$

where σ is the fracture stress, 1.24 is a geometrical constant, and c is the crack size [25]. Determination of c is obtained through the relation

$$c = \sqrt{ab} \quad (2)$$

where a and b are the axes of the semi-elliptical critical flaw, as shown in Fig. 1.

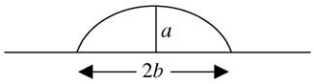

Figure 1 Determination of the critical flaw size, c, for a semi-elliptical flaw of axes a and $2b$.

2.3. Preparation of fibres for cell culture

Fibres were cut to approximately 1.5 cm length and attached to glass coverslips using agarose gel at either end of the fibres. Fibres were sterilised using UV light for 30 min and pre-incubated in Dulbecco's Modified Eagles Medium for 24 h prior to cell seeding.

2.4. Cell culture

Primary human osteoblast cells (HOBs) were isolated as described previously [26] from femoral heads after total hip-replacement surgery. Bone fragments of approximately 3 × 3 mm^2 were removed. Fragments were washed several times in phosphate buffered saline (PBS) to remove blood cells and debris with a final wash in culture medium. Fragments were then placed in tissue culture flasks in complete Dulbecco's modified eagles medium (DMEM) containing 10% Foetal Bovine Serum (FBS) with 1% glutamine, 2% penicillin/streptomycin, and 0.85 mM ascorbic acid. The fragments were incubated at 37 °C in a humidified incubator with 5% CO_2. Medium was changed every two days and after approximately four weeks in culture, bone fragments were discarded and cells harvested using trypsin EDTA. Cells were seeded onto fibres or seeded onto Thermanox discs as positive controls, at a density of 40 000 $cells/cm^2$.

2.5. Confocal microscopy

After culture for various time periods samples were washed twice in PBS and fixed in 4% paraformaldehyde for 10 min at room temperature. Samples were then washed in PBS and permeabilised in 0.2% Triton X-100 in PBS for 5 min at −20 °C. Samples were then washed in PBS containing 0.1% bovine serum albumin (PBS/BSA) and stained using Alexa Fluor 488 phalloidin (Molecular Probes) at a concentration of 40 U/ml (according to manufacturer recommendations) for 20 min at room temperature. Samples were washed in PBS/BSA and counterstained with propidium iodide at a concentration of 5 μg/ml in PBS for 30 s at room temperature. Samples were washed several times, placed onto glass slides and mounted under coverslips using PBS/glycerol mountant (1 : 1). Samples were then viewed using a BioRad MRC 600 confocal microscope.

2.6. Scanning electron microscopy

After culture for various time periods samples were washed twice in PBS and fixed in 3% glutaraldehyde in 0.1 M phosphate buffer for 30 min at 4 °C. Samples were washed in phosphate buffer and post-fixed in osmium tetraoxide for 1 h at 4 °C. Samples were washed again in phosphate buffer and dehydrated through a series of ethanol. After the final dehydration in 100% ethanol,

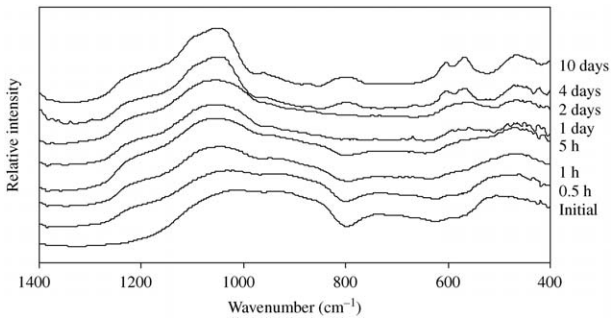

Figure 2 FTIR spectra of 20 μm bioactive 45S5 fibres following immersion in SBF. Crystalline HA formed after four days, as indicated by dual crystalline peaks near 604 and 565 cm^{-1}.

samples were transferred to hexamethyldisilazane (HMDS), a chemical drying agent for 5 min. Samples were then rinsed in fresh HMDS and left in a fumehood to allow complete drying. Samples were sputter coated with gold–palladium and viewed under a Cambridge stereoscan S360 scanning electron microscope at 10 kV.

3. Results

3.1. Bioactivity testing

The FTIR spectra of 20 μm diameter 45S5 fibres following 0.5 h to 10 days immersion in SBF are shown in Fig. 2. The initial spectrum is shown as well. No significant deviation from the initial spectrum was evident up to 5 h. However, after one day a broad P–O bend peak near 600 cm^{-1} is present, indicating the formation of an amorphous calcium phosphate surface layer [27]. The 2d spectra appeared similar to that following one day immersion. After four and 10 days immersion, a crystalline HA layer was evidenced by dual sharp peaks located near 604 and 565 cm^{-1} [27–29].

Fourier transform infrared spectroscopy spectra of the larger (40 μm) 45S5 fibres are shown in Fig. 3. After two days immersion, crystalline HA was formed on the fibre surfaces, as indicated by the presence of dual P–O bending peaks at 604 and 565 cm^{-1}. This HA also became slightly more crystalline with time (up to 10 days) as indicated by the further splitting of the P–O peaks.

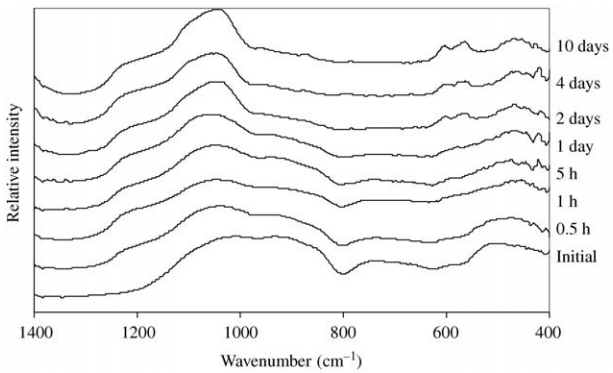

Figure 3 FTIR spectra of 40 μm bioactive 45S5 fibres following immersion in SBF. Crystalline HA was observed to form after two days, as indicated by dual crystalline peaks near 604 and 565 cm^{-1}.

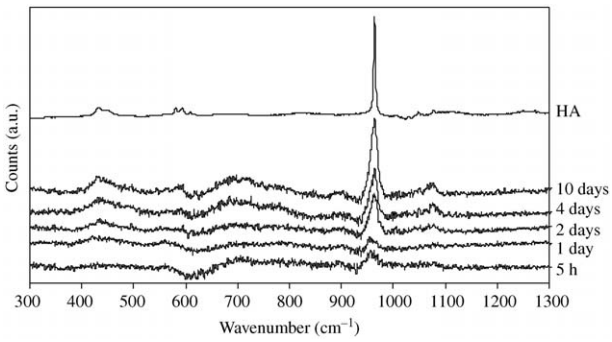

Figure 4 Difference Raman spectra of 45S5 fibres following 5 h to 10 days immersion in SBF. The HA reference is also shown.

Raman spectroscopic analysis of 40 μm fibres after 5 h, one, two, four, and 10 days is shown in Fig. 4. The spectra were normalised to show the difference between the raw Raman spectra taken at the labelled time period and the preceding period (0 h for the 5 h spectra). A spectrum of HA is also shown for comparison. The PO_4^{3-} peak at 964 m^{-1} increased with increasing immersion time, as the HA layer grew in thickness. The greatest increase in the PO_4^{3-} peak, observed after two days (Fig. 4), corresponded with the appearance of crystalline HA detected using FTIR (Fig. 3). Peaks near 460 and 610 cm^{-1} developed at four and 10 days, respectively, indicate a maturation of the HA layer.

3.2. Strength and toughness

The average failure stress $(n = 44)$ of hand-drawn 45S5 fibres was 340 $\pm$ 140 MPa (79 $\pm$ 19 μm diameter). The fracture surface of a 45S5 fibre fractured in tension is shown in Fig. 5. Twist-hackle marks point back towards the location of the critical flaw (indicated by an arrow in Fig. 5). The average $(n = 4)$ flaw size, c, was 2.0 $\pm$ 1.1 μm. The average fracture toughness (Equation 1), determined from the flaw size measurements (Equation 2) and the respective fracture stress values, was 0.7 ± 0.1 MPa m$^{1/2}$.

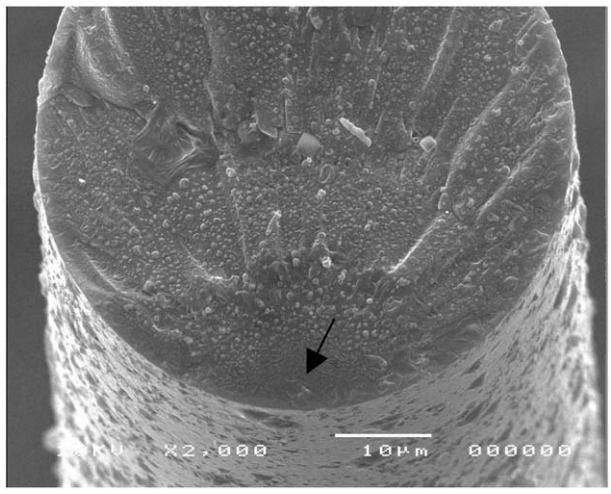

Figure 5 Fracture surface of 45S5 bioactive glass fibre. Twist-hackle marks are observed, which point back to the origin (shown by arrow). The average failure stress was 340 $\pm$ 140 MPa for fibres 79 $\pm$ 19 μm in diameter. The fracture toughness (K_{IC}), determined by fractographic methods, was 0.7 ± 0.1 MPa m$^{1/2}$.

3.3. Cell culture

Confocal microscopy was used to observe that human osteoblasts attached and spread rapidly after 15, 60 and 90 min in culture (Fig. 6). The fibres, which appear red in Fig. 6, were 40 μm in diameter. In these images, the cell body appears green due to the phalloidin (green) stain for F-actin, and the nucleus appears red owing to propidium iodine staining. In Fig. 6(a) osteoblasts are seen to attach to fibres after only 15 min in culture. At 30 min, a greater concentration of osteoblasts on the fibres surface was evident (Fig. 6(b)). Again, after 90 min, a larger number of spread cells was observed along with cell projections.

Osteoblasts remained attached and spread on the fibres at longer time-periods (up to 14 days). Fig. 7(a) shows a cell projection after 72 h in culture. A ruffled cell membrane was also visible. Fig. 7(b) shows a spread cell after 14 days in culture. Lamellipodia were visible, as were dorsal ruffles. Cracks in the fibre were as a result of the dehydration process after culture.

4. Discussion

Although the *in vitro* bioactivity of many forms of 45S5 glass has been characterised, published data on fibres is sparse [23]. In this study, the bioactive response, strength, and toughness, and preliminary osteoblast adhesion, attachment and spreading to 45S5 bioactive glass fibres was studied. FTIR spectroscopy was used to show that 40 and 20 μm 45S5 fibres formed HA surface layers following immersion in simulated body fluid after two and four days, respectively. After two days an amorphous layer of calcium phosphate was present on the 20 μm fibre surface as indicated by FTIR. Given that the SA : V ratio and other testing parameters for the 20 and 40 μm tests were equal, the difference in crystalline HA formation time is likely due to the presence of a silane coupling agent present on the 20 μm fibres.

Formation of HA on the fibre surface after two to four days was similar to other reported rates in the literature. For example, Orefice *et al*. [17] reported 77S sol–gel fibres formed HA after two days in SBF and Marcolongo

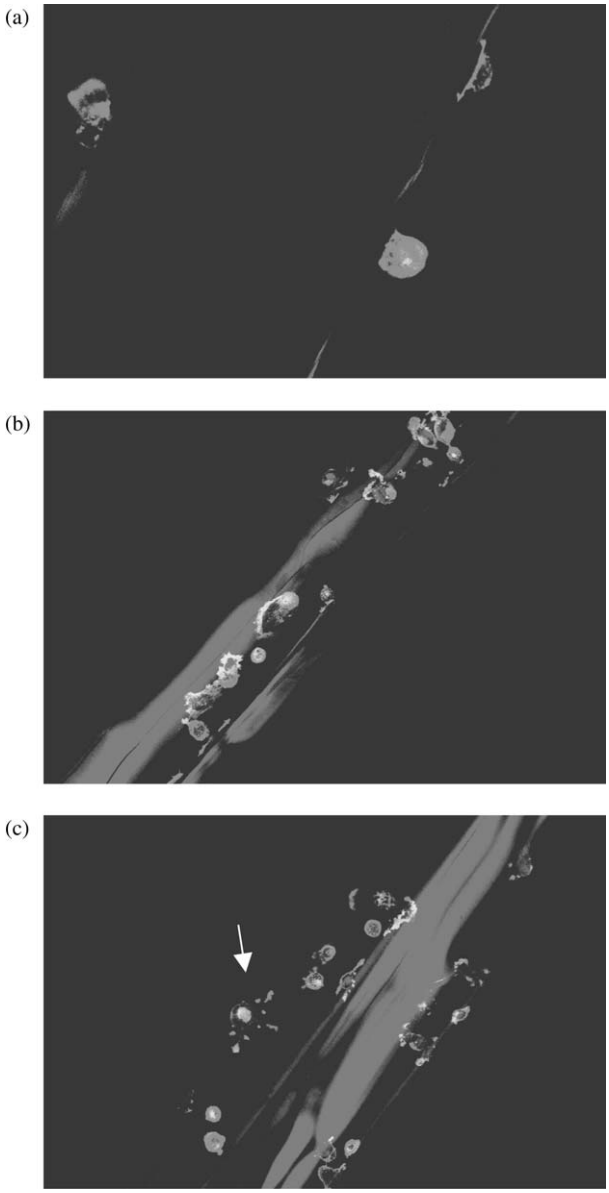

Figure 6 Confocal microscopy images of human osteoblasts cultured on 45S5 glass fibres after (a) 15 min, (b) 30 min, and (c) 90 min. Nuclei were stained with propidium iodide and F-actin was stained with FITC-conjugated phalloidin. Filopodia were observed extending from the main cell body (arrow).

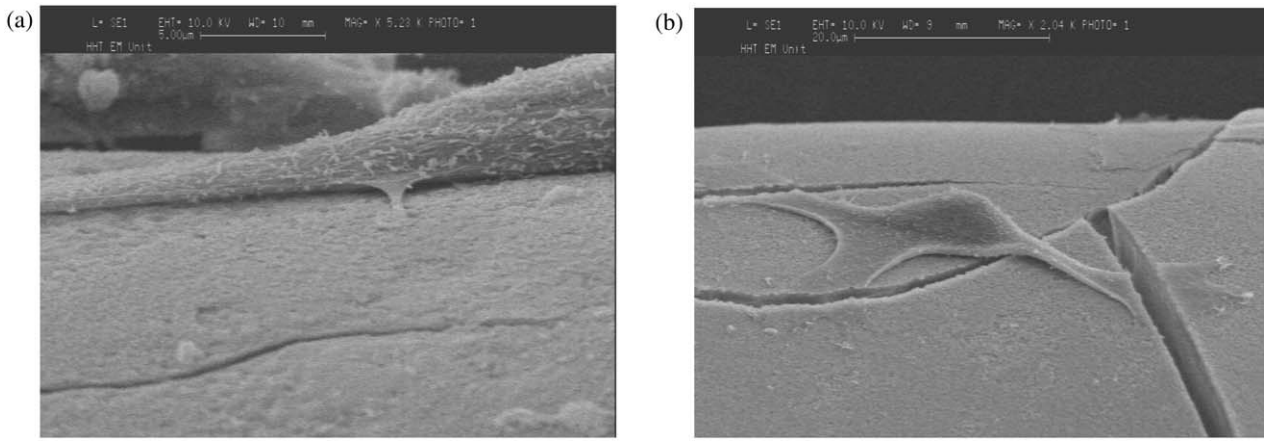

Figure 7 SEM micrographs of human osteoblasts on 45S5 fibres surfaces after (a) 72 h and (b) 14 days. A focal adhesion and a ruffled dorsal surface were present (a) as were cell projections (b). Cracking of the fibres was due to ethanol dehydration procedure for SEM.

et al. [21] reported the formation of HA after 10 days for an alumina containing silica based glass fibre.

Raman micro-spectroscopy proved to be sensitive to monitoring the formation of HA on the 45S5 fibre surface. The major peak at 960 cm^{-1} corresponded to the P–O symmetric stretching vibrations in PO_4^{3-} groups in HA. Increases of this peak with time (Fig. 3) could be used to chart the growth of the surface layer. The formed layer was shown to become more like stoichiometric HA with time. Similar maturation of the HA-like layer with time was reported for crystallised 45S5 particulate compacts [30]. The correlation between Raman and FTIR spectra with regard to bioactivity is potentially very valuable, because Raman analysis can be used to monitor the bioactivity of samples *in situ*. This is due to the insensitivity of Raman spectra to the presence of water, whereas water strongly absorbs portions of the FTIR spectral region.

The tensile strength of the 79 μm (average) diameter 45S5 fibres was 340 $\pm$ 140 MPa. Such results correspond well with the results of De Diego *et al*. [23], who found that tensile strengths of 200 and 300 μm 45S5 fibres were 200 and 150 MPa, respectively. As the fibre strength is a function of the flaw size (also a function of the fibre diameter) higher strength is expected, the smaller the fibre.

Fracture surface analysis was used to show that the critical flaw could be located and measured in 45S5 bioactive glass fibres. The fracture toughness, calculated by fracture surface analysis, was $0.7 \pm 1\ MPa\ m^{1/2}$. As toughness is a material property, it is not a function of the fibre diameter. Such results are reasonable for a silica based fibre. A fracture toughness of $0.6\ MPa\ m^{1/2}$ was previously reported for monolithic 45S5 bioactive glass [31].

Initial attachment of osteoblasts to the 45S5 fibre surface was studied using confocal microscopy. After 15 min in culture osteoblasts were observed to be present on 45S5 fibres showing rapid onset of cell adhesion. The number of cells was shown to increase at 30 min and then again at 90 min. After 90 min, filopodia were apparent indicating that osteoblasts were attaching and spreading onto the fibre surface. SEM revealed cell projections and dorsal ruffles of cells at higher magnification and for longer culture times. In this initial study of osteoblast responses, we demonstrated rapid cell attachment and spreading to the fibre surfaces. Such results are promising in that the level of osteoblast attachment and spreading is important in the long-term functions and phenotype of the cell. Further investigations are underway to analyse cell proliferation, matrix formation, mineralisation, and gene expression.

5. Conclusions

Fourier transform infrared spectroscopy analysis revealed that 45S5 glass fibres formed crystalline HA layers in two to four days *in vitro* using SBF. Raman micro-spectroscopy was also used to monitor the HA layer formation through assessment of the intensity increase of the PO_4^{3-} peak near 960 cm^{-1}. The greatest increase in the 964 cm^{-1} Raman peak correlated well with the appearance of crystalline HA using FTIR. Such results are encouraging for the *in situ* monitoring of *in vitro* fibre bioactivity, as Raman spectra are insensitive to the presence of water, unlike FTIR. The average 45S5 fibre tensile strength (79 μm diameter) was 340 $\pm$ 140 MPa. Fracture surface analysis was used to determine the fracture toughness of the bioactive 45S5 glass fibres was $0.7 \pm 0.1\ MPa\ m^{1/2}$. Osteoblasts attached and spread to the 45S5 fibre surface after 15–90 min, as determined by confocal microscopy. SEM also showed that cells remained attached after 14 days.

Acknowledgments

The authors gratefully acknowledge funding from DARPA and the March of Dimes charity. We would also like to acknowledge Mrs Margaret Mobberley and Dr Tim Ryder (The Electron Microscopy Unit, Department of Histopathology) for their assistance with the SEM.

References

1. T. B. LOVELACE, J. T. MELLONIG, R. M. MEFFERT, A. A. JONES, P. V. NUMMIKOSKI and D. L. COCHRAN, *J. Periodontol*. **69** (1998) 1027.
2. C. SHAPOFF, D. C. ALEXANDER and A. E. CLARK, *Compendium* **18** (1997) 352.
3. J. S. ZAMET, U. R. DARBAR, G. S. GRIFFITHS, J. S. BULMAN, U. BRAGGER, W. BURGIN and H. N. NEWMAN, *J. Clin. Periodontol*. **24** (1997) 410.
4. E. SCHEPERS, M. DECLERCQ and P. DUCHEYNE, *J. Oral Rehabil*. **18** (1991) 439.
5. D. L. WHEELER, *J. Biomed. Mater. Res*. **41** (1998) 527.
6. L. L. HENCH, R. J. SPLINTER, W. C. ALLEN and T. K. GREENLEE, *J. Biomed. Mater. Res. Symp*. **2** (1971) 117.
7. M. R. T. FILGUERIAS, G. LATORRE and L. L. HENCH, *J. Biomed. Mater. Res*. **27** (1993) 445.
8. D. C. GREENSPAN, J. P. ZHONG and G. P. LATORRE, in Proceedings of the 7th International Symposia on Ceramics in Medicine, Turku, Finland, 1994, pp. 55–60.
9. I. D. XYNOS, M. J. V. HUKKANEN, J. J. BATTEN, L. D. K. BUTTERY, L. L. HENCH and J. M. POLAK, *Calcif. Tissue Int*. **67** (2000) 321.
10. T. MATSUDA and J. E. DAVIES, *Biomaterials* **8** (1987) 275.
11. E. A. B. EFFAH KAUFMANN, P. DUCHEYNE and I. M. SHAPIRO, *J. Biomed. Mater. Res*. **52** (2000) 783.
12. E. A. B. EFFAH KAUFMANN, P. DUCHEYNE and I. M. SHAPIRO, *Tiss. Engr*. **6** (2000) 19.
13. I. D. XYNOS, A. J. EDGAR, L. D. K. BUTTERY, L. L. HENCH and J. M. POLAK, *Biochem. Biophys. Res. Comm*. **276** (2000) 461.
14. I. D. XYNOS, A. J. EDGAR, L. D. K. BUTTERY, L. L. HENCH and J. M. POLAK, *J. Biomed. Mater. Res*. **55** (2001) 151.
15. T. PELTOLA, M. JOKINEN, S. VEITTOLA, H. RAHIALA and A. YLI-URPO, *Biomaterials* **22** (2001) 589.
16. T. PELTOLA, M. JOKINEN, S. VEITTOLA, J. SIMOLA and A. YLI-URPO, *J. Biomed. Mater. Res*. **54** (2001) 579.
17. R. L. OREFICE, L. L. HENCH, A. E. CLARK and A. B. BRENNAN, *ibid*. **55** (2001) 460.
18. R. Z. DOMINGUES, A. E. CLARK and A. B. BRENNAN, *ibid*. **55** (2001) 468.
19. P. L. CLAPP, M.S. Thesis, Alfred University, New York (2001).
20. K. P. ANDRIANO, A. U. DANIELS and J. HELLER, *J. Appl. Biomat*. **3** (1992) 197.
21. M. MARCOLONGO, P. DUCHEYNE and W. C. LACOURSE, *J. Biomed. Mater. Res*. **37** (1997) 440.
22. D. C. CLUPPER, M. M. HALL, J. E. GOUGH and L. L. HENCH, in Transactions of the Society for Biomaterials 2002, Tampa, FL, 2002.
23. M. A. DE DIEGO, N. J. COLEMAN and L. L. HENCH, *J. Biomed. Mater. Res*. **53** (2000) 199.

24. T. KOKUBO, H. KUSHITANI, S. SAKKA, T. KITSUGI and T. YAMAMURO, *ibid*. **24** (1990) 721.
25. J. J. MECHOLSKY, JR., in ''Nucleation and Crystallization in Glasses. Advances in Ceramics'', Vol. 4, edited by J. H. Simmons, D. R. Uhlmann and G. H. Beall (The American Ceramic Society, Columbus, OH, 1982) p. 261.
26. J. E. WERGEDAL and D. J. BAYLINK, *Proceedings of the Society for Experimental Biology and Medicine* **176** (1984) 60.
27. M. R. T. FILGUERIAS, G. LATORRE and L. L. HENCH, *J. Biomed. Mater. Res.* **27** (1993) 1485.
28. C. Y. KIM, A. E. CLARCK and L. L. HENCH, *J. Non-Cryst. Solids* **113** (1989) 195.
29. C. OHTSUKI, H. KUSHITANI, T. KOKUBO, S. KOTANI and T. YAMAMURO, *J. Biomed. Mater. Res.* **25** (1991) 1363.
30. D. C. CLUPPER, J. J. MECHOLSKY JR., G. P. LATORRE and D. C. GREENSPAN, *ibid*. **57** (2001) 532.
31. I. D. THOMPSON and L. L. HENCH, *Proc. Inst. Mech. Engrs.* **212** (1998) 127.

Received 3 June 2003
and accepted 21 January 2004